

Scattering resonances and background associated with an asymmetric potential barrier via Siegert pseudostates

Valentin N. Ostrovsky*

V. Fock Institute of Physics, St. Petersburg State University, 198504 St. Petersburg, Russia

Nils Elander†

Stockholm University, Department of Physics, Alba Nova University Center, SE-106 91 Stockholm, Sweden

(Received 16 September 2004; published 17 May 2005)

The transmission of a nonsymmetric potential barrier is a two-channel quantum problem. In this aspect it is analogous to the two-channel radial problem. The analytical properties of the S matrix are similar for both generic quantum-mechanical systems. We here develop an explicit mapping between the two problems. It allows us to formulate barrier transmission in terms of the Siegert pseudostates similarly to the approach developed recently for the two-channel radial case. This results in an efficient method of treating barrier transmission including on equal footing both resonance effects and smooth background behavior.

DOI: 10.1103/PhysRevA.71.052707

PACS number(s): 34.10.+x, 34.50.Lf

I. INTRODUCTION

In this study we carry out a comparative analysis of two generic problems in quantum mechanics. One of them is the two-channel (TC) radial problem described by a set of two coupled equations

$$\begin{aligned} -\frac{1}{2} \frac{d^2 \psi_1}{dr^2} + V_{11}(r) \psi_1 + V_{12}(r) \psi_2 &= E \psi_1, \\ -\frac{1}{2} \frac{d^2 \psi_2}{dr^2} + V_{22}(r) \psi_2 + V_{21}(r) \psi_1 &= E \psi_2. \end{aligned} \quad (1)$$

The wave function here has two components $\psi_1(r)$ and $\psi_2(r)$ defined on the semiaxis $0 \leq r < \infty$ and subject to the boundary condition $\psi_1(0) = \psi_2(0) = 0$. The potential matrix $V_{ij}(r)$ is real and symmetric and for large r has the asymptote $V_{ij}(r) = v_i \delta_{ij}$ where the constants v_1 and v_2 are threshold energies.

The other problem is the one-dimensional barrier transmission (BT) described by a Schrödinger equation for a single function $\psi(x)$ considered on the entire axis $-\infty < x < \infty$,

$$(H - E)\psi(x) = 0, \quad H = -\frac{1}{2} \frac{d^2}{dx^2} + V(x). \quad (2)$$

The potential function $V(x)$ generally is asymmetric and, in particular, has different limits for $x \rightarrow \pm\infty$: $V(x)|_{x \rightarrow -\infty} = v_1$ and $V(x)|_{x \rightarrow \infty} = v_2$.

The importance of the two problems for quantum mechanics and their application does not require an extended substantiation. We here only stress that resonance effects in BT play an important role in semiconductors and that the BT problem represents the simplest and most frequently used model of chemical reactions. In this application x plays the role of an effective reaction coordinate.

Apparently quite different, the TC and BT problems have an important common feature: they are two-channel problems with channel threshold energies v_1 and v_2 . This implies a number of common general properties intrinsic for the two-channel problems. From the standpoint of an approach based on analytical properties of the scattering matrix, or Green function, the common features arise from the basic fact that the plane of complex energy E has two square-root branch points v_1 and v_2 . Respectively, the complex energy plane has four Riemann sheets. This is clear from the fact that in both cases the essential variables are the channel momenta $k_{1,2} = \sqrt{E - v_{1,2}}$. To the best of our knowledge this quite evident observation was not duly emphasized before, to say nothing about its practical use. The sort of analytical isomorphism of the two problems suggests a possibility of some mapping of one problem onto other, although a convenient concrete way to implement this general idea is not obvious at first sight. In order to illustrate the difficulties it is sufficient to indicate that the TC problem is characterized by essentially three potential functions $V_{11}(r)$, $V_{22}(r)$, and $V_{12}(r) = V_{21}(r)$ of the radial variable r ($0 \leq r < \infty$), whereas in BT one finds a single potential $V(x)$ defined on the entire axis $-\infty < x < \infty$.

The objective of the present study is to implement mapping based on the discretized representation in terms of the Siegert pseudostates. The Siegert pseudostates approach was developed at first for the one-channel radial problem [1,2] where it was demonstrated as a convenient and quite universal tool. Subsequently the TC radial problem was thoroughly analyzed along these lines [3]. The mapping allows us to transfer these results, with proper modifications, to the BT problem. The full analysis of the BT problem in terms of Siegert pseudostates has not yet been carried out, although the case of symmetric barriers was considered in relation to the theory of cumulative reaction probability [4]. The symmetric barrier in terms of the two-channel problem implies a degeneracy of channel thresholds which is a particular subset of the general situation. It requires a special technical treatment being reducible to a set of two one-channel problems as shown in Ref. [4]; probably the issue deserves more attention

*Electronic address: Valentin.Ostrovsky@pobox.spbu.ru

†Electronic address: elander@physto.se

in application to the barrier transmission problem, but we postpone its analysis to the future. It is worthwhile here to stress the terminology used below. The case of a symmetric barrier should be distinguished from the more general case of threshold degeneracy. Any symmetric barrier is necessarily degenerate, but degeneracy generally might also occur for nonsymmetric barriers.

The mapping developed below (Sec. II) demonstrates how the BT problem is formulated in terms of Siegert pseudostates. Besides its general interest this is a pragmatically useful representation effective for a quantitative description of resonance effects. The Siegert representation for the BT coefficient conveniently includes both the resonance effects and smooth background variation. This is an important aspect, since, as already indicated, the BT problem is a generic model for a variety of complicated processes in quantum physics.

Now to our demonstration example (Sec. III): the individual Siegert states for a BT problem were considered in Refs. [5–7]. The Siegert poles were located there by using the method of complex coordinate rotation. The particularly refined calculations of Ref. [7] report the position of 45 Siegert poles. The symmetric model potential considered had two humps with a dip between them. It is able to support bound states as well as resonances. The generalized form (43) of this potential is used below in our illustrative calculations. Later the cumulative reaction probability was evaluated [8] in terms of Siegert states, but only for the special case of the exactly solvable model of the Eckart potential. Using the nonsymmetric Eckart potential the authors were able to analyze a model problem with nondegenerate thresholds. Note, however, that the cumulative reaction probability was expressed via Siegert poles only for the symmetric version, and thus the analytical features of the nondegenerate two-channel problem did not appear. Moreover, all the construction was substantially based on the exact analytical solution available for the Eckart potential without the possibility of generalization. The rigidity of the exactly solvable model led to substantial physical restrictions: a purely repulsive potential did not permit consideration of resonance effects. Later Siegert states appeared in a number of publications on the BT problem [9–12]. Besides the coordinate complex rotation method [5–7,10], direct integration of the Schrödinger equation was employed to locate their positions [9,12].

In the aspect of modeling chemical reactions the symmetrical (as well as nonsymmetrical but degenerate) model looks unnecessarily restrictive, since the chemical reactions of interest normally do not correspond to the energy resonance between reagents and products. Nonetheless, the BT problem for general nonsymmetric potentials attracted much less attention in the literature compared to the symmetrical version. To the best of our knowledge we are not aware of any previous calculations of resonances for the asymmetric potential, although for symmetrical and/or degenerate cases similar calculations are quite abundant (see the papers cited above). This means that the material for numerical comparison and testing of the results is absent.

It can be noted that more complicated BT models with two interacting potential curves were studied recently quite extensively within the scattering calculation approach, in-

cluding resonance effects [13–15]. However, accurate calculations of resonance, for instance, within the complex dilation approach, are not known for this model. Note that the problem of two interacting potential curves on the axis $-\infty < x < \infty$ generally corresponds to the four-channel problem, with a more complicated analytical structure than in the two-channel case considered in the present study.

II. TRANSMISSION THROUGH A BARRIER IN THE GENERAL NONDEGENERATE CASE

A. Green function and S matrix

Suppose that the potential energy $V(x)$ is constant when x lies outside interval $a_1 < x < a_2$:

$$V(x) = v_1, \quad x < a_1,$$

$$V(x) = v_2, \quad x > a_2. \quad (3)$$

Then solutions of Eq. (2) outside this interval correspond to plane waves with wave numbers k_1, k_2 :

$$E = v_1 + \frac{1}{2}k_1^2 = v_2 + \frac{1}{2}k_2^2. \quad (4)$$

As already indicated, the parameters v_1 and v_2 have the meaning of channel thresholds.

The outgoing-wave Green function $G(x, x')$ obeys the equation

$$\left[-\frac{1}{2} \frac{d^2}{dx^2} + V(x) - E \right] G(x, x') = \delta(x - x'), \quad (5)$$

with boundary conditions

$$\left(\frac{d}{dx} + ik_1 \right) G(x, x') = 0, \quad x < a_1, \quad x < x', \quad (6)$$

$$\left(\frac{d}{dx'} - ik_2 \right) G(x, x') = 0, \quad x' > a_2, \quad x' > x. \quad (7)$$

The scattering matrix is defined via the solution of the Schrödinger equation $\psi_{\pm}(x)$ with appropriate normalization:

$$\psi_+(x) = \frac{1}{\sqrt{k_1}} \exp(ik_1 x) + S_{11} \frac{1}{\sqrt{k_1}} \exp(ik_1 x), \quad x < a_1,$$

$$\psi_+(x) = S_{12} \frac{1}{\sqrt{k_2}} \exp(ik_2 x), \quad x > a_2, \quad (8)$$

$$\psi_-(x) = S_{21} \frac{1}{\sqrt{k_1}} \exp(-ik_1 x), \quad x < a_1,$$

$$\psi_-(x) = \frac{1}{\sqrt{k_2}} \exp(-ik_2 x) + S_{22} \frac{1}{\sqrt{k_2}} \exp(ik_2 x), \quad x > a_2. \quad (9)$$

By direct calculations the S matrix could be straightforwardly related to the Green function:

$$S_{11} = -\exp(2ik_1a_1)[1 + ik_1G(a_1, a_1)], \quad (10)$$

$$S_{22} = -\exp(-2ik_2a_2)[1 + ik_2G(a_2, a_2)], \quad (11)$$

$$S_{12} = -i\sqrt{k_1k_2}\exp(ik_1a_1 - ik_2a_2)G(a_1, a_2), \quad (12)$$

$$S_{21} = -i\sqrt{k_1k_2}\exp(ik_1a_1 - ik_2a_2)G(a_1, a_2). \quad (13)$$

B. Siegert states

The Siegert states $\phi(x)$ are conventionally defined as solutions of the Schrödinger equation (2) that satisfy outgoing-wave boundary conditions

$$\left. \left(\frac{d}{dx} + ik_1 \right) \phi(x) \right|_{x=a_1} = 0, \quad (14)$$

$$\left. \left(\frac{d}{dx} - ik_2 \right) \phi(x) \right|_{x=a_2} = 0.$$

Such solutions exist only for discrete values of the energy E_n . The energies E_n are generally complex valued and correspond to poles of the S matrix or Green function.

C. Discretization and Siegert pseudostates

We introduce a finite real basis

$$\pi_m(x), \quad m = 1, 2, \dots, N, \quad (15)$$

which is orthonormal in the interval $a_1 < x < a_2$:

$$\int_{a_1}^{a_2} \pi_m(x) \pi_n(x) dx = \delta_{mn}. \quad (16)$$

We expand the Siegert state over this basis,

$$\phi(x) = \sum_{n=1}^N c_n \pi_n(x), \quad (17)$$

and substitute the expansion into Eq. (2) to obtain the matrix equation

$$\left(\tilde{\mathbf{H}} - \frac{i}{2}k_1\mathbf{L}_1 - \frac{i}{2}k_2\mathbf{L}_2 - E\mathbf{I} \right) \mathbf{c} = 0. \quad (18)$$

Here we introduced N -component column vector $\mathbf{c} = \{c_1, c_2, \dots, c_N\}$ and $N \times N$ symmetric matrices $\tilde{\mathbf{H}}, \mathbf{L}_1, \mathbf{L}_2$:

$$\tilde{H}_{ij} = \frac{1}{2} \int_{a_1}^{a_2} \frac{d\pi_i(x)}{dx} \frac{d\pi_j(x)}{dx} dx + \int_{a_1}^{a_2} \pi_i(x) V(x) \pi_j(x) dx, \quad (19)$$

$$(L_1)_{ij} = \pi_i(a_1) \pi_j(a_1), \quad (L_2)_{ij} = \pi_i(a_2) \pi_j(a_2). \quad (20)$$

\mathbf{I} is an $N \times N$ unit matrix.

In the case when the basis $\pi_j(x)$ is nonorthogonal, with the overlap matrix \mathbf{W} ,

$$W_{ij} = \int_{a_1}^{a_2} \pi_i(x) \pi_j(x) dx, \quad (21)$$

formula (18) is generalized to

$$\left(\tilde{\mathbf{H}} - \frac{i}{2}k_1\mathbf{L}_1 - \frac{i}{2}k_2\mathbf{L}_2 - E\mathbf{W} \right) \mathbf{c} = 0. \quad (22)$$

Equation (18) or (22) formulates a nonlinear eigenvalue problem for the spectral parameter: the energy E and related eigenvector \mathbf{c} . It is *exactly* linearized by using uniformization and quadrupling the dimension of the Hilbert space, N .

D. Uniformization of the barrier transmission problem

Equation (18) or (22) is a nonlinear (irrational) eigenvalue problem, since it contains E , k_1 , and k_2 connected by the energy conservation relation (4). The uniformization procedure [17] makes the problem rational in terms of the variable u defined on a single Riemann sheet in the complex u plane:

$$E = \bar{v} - q^2 \frac{1+u^4}{2u^2}, \quad (23)$$

$$q = \sqrt{\frac{v_2 - v_1}{2}}, \quad \bar{v} = \frac{v_1 + v_2}{2}, \quad (24)$$

$$k_1 = iq \frac{u^2 - 1}{u}, \quad k_2 = iq \frac{u^2 + 1}{u}. \quad (25)$$

Then Eq. (18) is recast as

$$(\mathbf{I} + u\mathbf{B}^- + u^2\mathbf{A} + u^3\mathbf{B}^+ + u^4\mathbf{I}) \mathbf{c} = 0, \quad (26)$$

$$\mathbf{B}^+ = \frac{1}{q}(\mathbf{L}_1 + \mathbf{L}_2), \quad \mathbf{B}^- = \frac{1}{q}(-\mathbf{L}_1 + \mathbf{L}_2), \quad \mathbf{A} = \frac{2}{q^2}(\tilde{\mathbf{H}} - \bar{v}\mathbf{I}). \quad (27)$$

Formally the BT problem equations (26) and (27) coincide with those obtained by Sitnikov and Tolstikhin [3] for the radial TC problem. Thus the mapping of two problems on each other is achieved. Both problems are characterized in a discrete-basis representation by three $N \times N$ matrices $\tilde{\mathbf{H}}, \mathbf{L}_1$, and \mathbf{L}_2 . Of course the physical meaning of these matrices is somewhat different. The dimensionality of the problems in the discretized representation is worthy of some attention. In the radial two-channel system the dimension of the nonlinear eigenvalue problem (26) is $(N_1 + N_2)$ where N_1 and N_2 are dimensions of bases used in the channels 1 and 2, respectively. In the barrier penetration problem the dimension N is the dimension of the basis (15) on the $-\infty < x < \infty$ axis.

For a nonorthogonal basis formula (26) is modified to

$$(\mathbf{W} + u\mathbf{B}^- + u^2\mathbf{A} + u^3\mathbf{B}^+ + u^4\mathbf{W}) \mathbf{c} = 0, \quad (28)$$

$$\mathbf{A} = \frac{2}{q^2}(\tilde{\mathbf{H}} - \bar{v}\mathbf{W}). \quad (29)$$

E. Relation between barrier transmission problem and radial two-channel problem

The formulation of the exactly linearized representation of the eigenvalue problem (26) coincides with formula (31) in Ref. [3]. Namely, the manifold of Siegert pseudopoles u_n (in terms of uniformization variable u) and related Siegert pseudostates $\mathbf{c}^{(n)}$ (in the discrete basis) is found as eigenvalues and eigenstates of the linear problem with dimension $4N$:

$$\begin{pmatrix} \mathbf{0} & \mathbf{W} & \mathbf{0} & \mathbf{0} \\ \mathbf{0} & \mathbf{0} & \mathbf{W} & \mathbf{0} \\ \mathbf{0} & \mathbf{0} & \mathbf{0} & \mathbf{W} \\ -\mathbf{W} & -\mathbf{B}^- & -\mathbf{A} & -\mathbf{B}^+ \end{pmatrix} \begin{pmatrix} \mathbf{c} \\ u\mathbf{c} \\ u^2\mathbf{c} \\ u^3\mathbf{c} \end{pmatrix} = u \begin{pmatrix} \mathbf{W} & \mathbf{0} & \mathbf{0} & \mathbf{0} \\ \mathbf{0} & \mathbf{W} & \mathbf{0} & \mathbf{0} \\ \mathbf{0} & \mathbf{0} & \mathbf{W} & \mathbf{0} \\ \mathbf{0} & \mathbf{0} & \mathbf{0} & \mathbf{W} \end{pmatrix} \begin{pmatrix} \mathbf{c} \\ u\mathbf{c} \\ u^2\mathbf{c} \\ u^3\mathbf{c} \end{pmatrix}. \quad (30)$$

We present here the equation for general case of a nonorthogonal basis. The special structure of eigenvectors shown in Eq. (30) is not a restrictive additional assumption, since it is easy to show that all eigenvectors automatically have such a structure.

Since the linearized problems are essentially the same for the BT and TC problems, the derivations of their corollaries in the discrete-basis representation coincide. Note, however, that the connection formulas (10) relating the S matrix and Green function contain exponents with a plus and minus in the arguments, whereas in the two-channel radial problem one always finds a plus. More differences in the formulas appear in the course of the transition to the coordinate representation.

For instance, the normalization condition is derived as in Ref. [3] and in the coordinate representation is

$$\int_{a_1}^{a_2} \phi_n(x)\phi_m(x)dx + i\frac{\phi_n(a_1)\phi_m(a_1)}{k_1^{(n)} + k_1^{(m)}} + i\frac{\phi_n(a_2)\phi_m(a_2)}{k_2^{(n)} + k_2^{(m)}} = \delta_{nm}. \quad (31)$$

Here $k_1^{(n)}$ and $k_2^{(n)}$ are expressed in terms of uniformization variable eigenvalues u_n via formulas (25).

The completeness relation reads

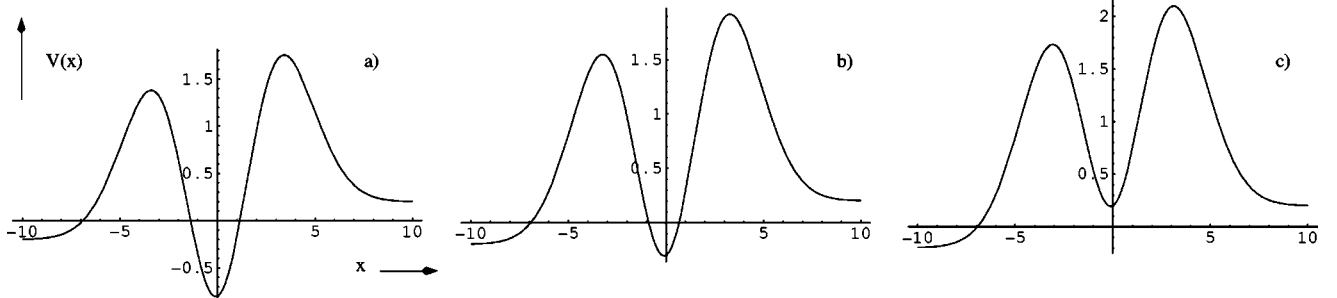


FIG. 1. The potentials in Eq. (43) with (a) $J=0.8$, (b) $J=0.3$, and (c) $J=-0.2$, respectively. Atomic units (a.u.) are used.

TABLE I. The energies for the optional bound state and lowest resonances obtained for various values of the potential parameter J , $s=0.1$, $\beta=0.5$, and $\Delta=0.2$ in Eq. (43). Atomic units (a.u.) are used.

J	$\text{Re}(E)$	$-\text{Im}(E)$
0.8	-0.320 597 26	0
	0.614 234 779	$1.548\ 704 \times 10^{-4}$
	1.313 607 466	$2.615\ 328 \times 10^{-2}$
	1.799 336 045	0.189 467
0.3	0.171 168 91	$4.141\ 506 \times 10^{-7}$
	1.026 959 39	$1.222\ 212 \times 10^{-3}$
	1.649 140 21	$6.073\ 172 \times 10^{-2}$
	2.078 474 00	0.276 736
-0.2	0.643 042 62	$9.141\ 66 \times 10^{-6}$
	1.429 909 65	$6.081\ 867 \times 10^{-3}$
	1.983 517 56	0.110 1469
	2.361 119 54	0.387 6087

$$\sum_{n=1}^{\infty} \phi_n(x)\phi_n(x') = 4\delta(x-x'). \quad (32)$$

The expressions for the Green function in terms of the Siegert pseudostates formally looks as related expressions (70) and (71) from Ref. [3] (within the obvious substitution $r \rightarrow x$):

$$G(x,x') = \frac{1}{q^2} \sum_{n=1}^{4N} \frac{u_n^3 \phi_n(x)\phi_n(x')}{(1-u_n^4)(u_n-u)}. \quad (33)$$

$$ik_1 G(x,x') = \frac{1}{q_{n=1}} \sum_{n=1}^{4N} \frac{u_n^2 \phi_n(x)\phi_n(x')}{(u_n^2+1)(u_n-u)}, \quad (34)$$

$$ik_2 G(x,x') = \frac{1}{q_{n=1}} \sum_{n=1}^{4N} \frac{u_n^2 \phi_n(x)\phi_n(x')}{(u_n^2-1)(u_n-u)}. \quad (35)$$

However, the implications are somewhat different. In the TS problem each Siegert pseudostate $\phi_n(r)$ is a vector function—i.e., a two-dimensional column vector with a component in each channel; respectively, the Green function is a 2×2 matrix. In the BT problem the Siegert pseudostate

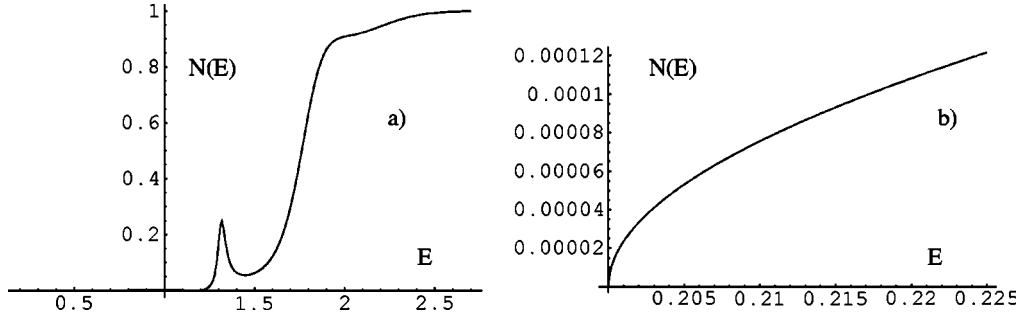


FIG. 2. (a) The overall view of the transmission coefficient $N(E)$ defined in Eq. (42) as a function of the energy E obtained for the potential (1) with $J=0.8$. (b) The characteristic threshold cusp is seen in the vicinity of the second channel threshold. Atomic units (a.u.) are used.

$\phi_n(x)$ and Green function $G(x, x')$ are plain (scalar) functions.

Useful expressions in terms of the Siegert pseudostates,

$$1 + ik_1 G(a_1, a_1) = \prod_{n=1}^{4N} \frac{1 - uu_n}{u - u_n}, \quad (36)$$

$$1 + ik_2 G(a_2, a_2) = \prod_{n=1}^{4N} \frac{1 + uu_n}{u - u_n}, \quad (37)$$

$$\begin{aligned} & [1 + ik_1 G(a_1, a_1)][1 + ik_2 G(a_2, a_2)] + k_1 k_2 [G(a_1, a_2)]^2 \\ &= \prod_{n=1}^{4N} \frac{u + u_n}{u - u_n}, \end{aligned} \quad (38)$$

are obtained from related TC formulas [3] by the replacement $G_{mn}(a, a) \Rightarrow G(a_m, a_n)$.

The expressions for the S -matrix elements might be cast in various forms:

$$\begin{aligned} S_{11} &= e^{2ik_1 a_1} \prod_{n=1}^{4N} \frac{1 - uu_n}{u - u_n} = e^{2ik_1 a_1} \prod_{n=1}^{4N} \frac{i}{2q} \frac{k_1 k_2^{(n)} + k_2 k_1^{(n)}}{k_1 - k_1^{(n)}} \\ &= e^{-2ik_1 a_1} \frac{1}{(2q)^{4N}} \prod_{n=1}^{4N} \frac{k_1 k_2^{(n)} + k_2 k_1^{(n)}}{k_1 - k_1^{(n)}}, \end{aligned} \quad (39)$$

$$\begin{aligned} S_{22} &= e^{-2ik_2 a_2} \prod_{n=1}^{4N} \frac{1 + uu_n}{u - u_n} = e^{-2ik_2 a_2} \prod_{n=1}^{4N} \frac{-i}{2q} \frac{k_1 k_2^{(n)} + k_2 k_1^{(n)}}{k_2 - k_2^{(n)}} \\ &= e^{-2ik_2 a_2} \frac{1}{(2q)^{4N}} \prod_{n=1}^{4N} \frac{k_1 k_2^{(n)} + k_2 k_1^{(n)}}{k_2 - k_2^{(n)}}, \end{aligned} \quad (40)$$

$$\begin{aligned} S_{12} &= e^{ik_1 a_1 - ik_2 a_2} \sqrt{\prod_{n=1}^{4N} \frac{1 - u^2 u_n^2}{(u - u_n)^2} - \prod_{n=1}^{4N} \frac{u + u_n}{u - u_n}} \\ &= e^{ik_1 a_1 - ik_2 a_2} \sqrt{\prod_{n=1}^{4N} \frac{1}{2q^2} \frac{(k_1 k_2^{(n)} + k_2 k_1^{(n)})^2}{(k_1 - k_1^{(n)})(k_2 - k_2^{(n)})} - \prod_{n=1}^{4N} \frac{k_1 + k_1^{(n)}}{k_2 - k_2^{(n)}}}. \end{aligned} \quad (41)$$

These formulas enable us to express the probability that a particle, with a total energy E , first located on one side of the barrier will appear on the other side. We define the transmission coefficient $N(E)$ as a function of the energy E as

$$N(E) = |S_{12}(E)|^2. \quad (42)$$

Additional information is contained in the phases of the scattering matrix elements $S_{jk}(E)$. Since it is less important physically, in our model examples below we consider only $N(E)$.

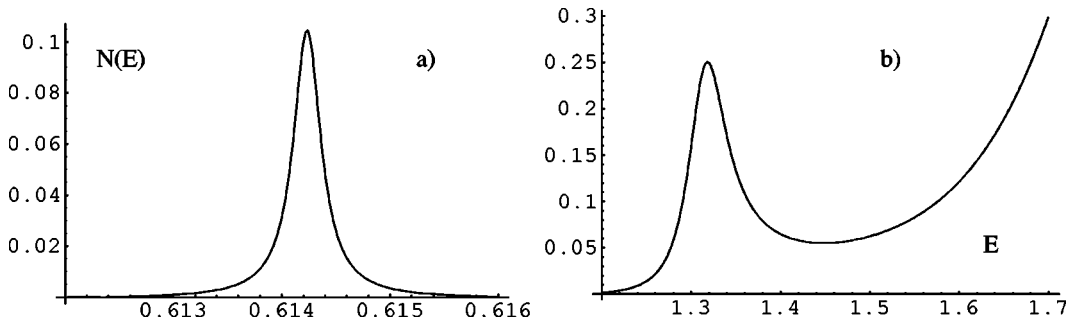


FIG. 3. Using $J=0.8$, we show (a) the transmission coefficient in the vicinity of the first resonance and (b) the transmission coefficient in the vicinity of the second resonance. Atomic units (a.u.) are used.

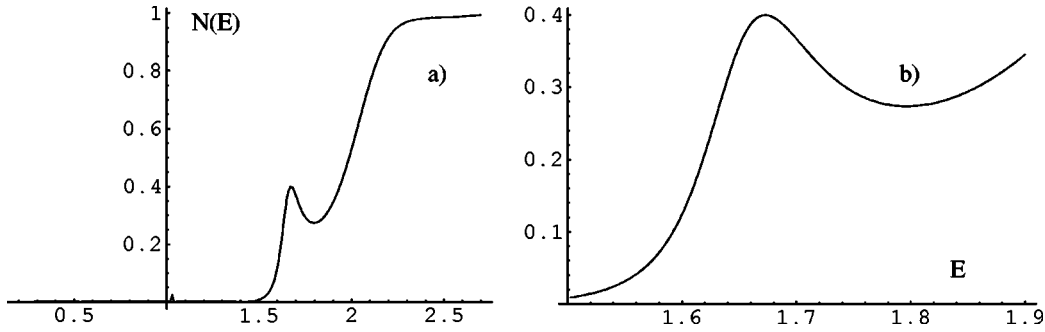


FIG. 4. (a) The overall view of the transmission coefficient $N(E)$ [from Eq. (42)] obtained for the potential (43) for $J=0.3$. (b) $N(E)$ in the vicinity of the third resonance. Atomic units (a.u.) are used.

III. MODEL ASYMMETRIC BARRIER POTENTIAL: CALCULATION AND RESULTS

To illustrate the theory above we use a nonsymmetrical double-hump potential capable of supporting bound states and resonances:

$$V(x) = \left(\frac{1}{2}x^2 - J \right) \exp(-sx^2) + \Delta \tanh(\beta x). \quad (43)$$

The parameter Δ is half difference of threshold energies being related to q introduced by formula (23) as $q = \sqrt{\Delta}$. The average threshold energy \bar{v} , Eq. (23), is zero, $\bar{v}=0$. In the degenerate case $\Delta=0$ the potential (43) is reduced to the model potential considered previously [5–7]. For the parameters s and β we keep values adopted in the cited publications, $s=0.1$, $\beta=0.5$. As for the parameter J , earlier it was chosen as $J=0.8$; in the present study we vary J (as in Table I) to see evolution of transmission coefficient pattern.

As a basis set $\pi_m(x)$ we employed a finite-element basis as used in Ref. [16] (note that we do not carry out complex coordinate dilation as in the cited paper). We tested that for small threshold splittings Δ and $J=0.8$ the positions of the first Siegert pseudostates approach results obtained for the degenerate case [7]. In the subsequent calculations we employed a relatively large parameter $\Delta=0.2$. Thus the threshold splitting is equal to 0.4. The barrier penetration now starts from the energy above $E=0.2$ (we recall that the energy zero is chosen halfway between the channel thresholds).

The potentials for various values of J are displayed in Fig. 1. The energies of the first bound state(s) (if any) and resonances obtained with these potentials are given in Table I.

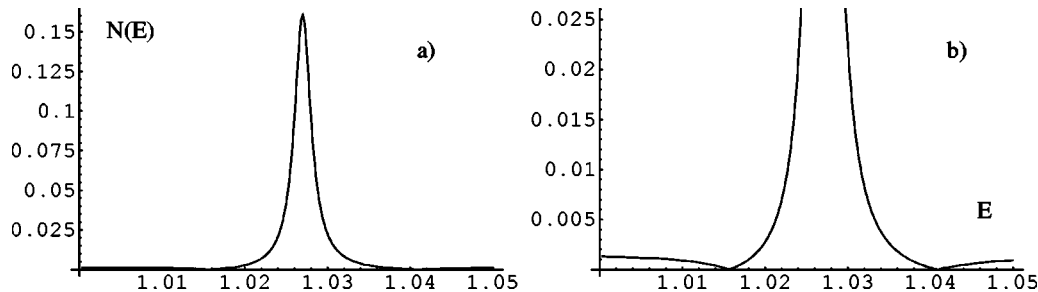


FIG. 5. Using $J=0.3$ we display (a) the transmission coefficient in the vicinity of the first resonance and (b) a closer look. Atomic units (a.u.) are used.

The overall energy dependence of the transmission coefficient $N(E)$ related to the left potential in Fig. 1 ($J=0.8$) is shown in the left part of Fig. 2. This potential supports one bound state with $E=-0.303$, as shown in the table. The lowest resonances lie at $E_1=0.614$, $E_2=1.314$, and $E_3=1.799$. Note also the characteristic cusp behavior in the transmission coefficient $N(E)$ in the vicinity of the second threshold $E=0.2$, as shown in the right part of Fig. 2.

We show the vicinities of the first and second resonances in Fig. 3. The first of them is so narrow that it is not noticeable in the overall view in Fig. 2. The other examples of very narrow resonances are presented in Figs. 5 and 7 below. The location of such narrow resonances within the scattering calculations would pose a problem, but within the Siegert pseudostates formulation they are located immediately.

On the other hand, the influence of the second resonance E_2 is clearly seen even in the overall view (Fig. 2) as a relatively sharp peak; it is detailed in the right part of Fig. 3. The third resonance E_3 apparently is the origin of the hump around $E=1.8$ in Fig. 2.

As the potential parameter J decreases, the bound state is pushed out into the continuum. The potential for $J=0.3$, as displayed in middle of Fig. 1, already does not support any bound state. We have here computed four resonances (see Table I) of which the lowest, $E_1=0.0171$, is in the lowest continuum, below the second energy threshold. This means that it decays with particle emission only in the left but not in the right direction. Such a resonance is not manifested in the transmission coefficient $N(E)$ [although it induces step-like behavior of the elastic scattering phase—i.e., half-phase of the matrix element $S_{11}(E)$]. In the overall transmission coefficient, which is displayed in the left of Fig. 4, we barely

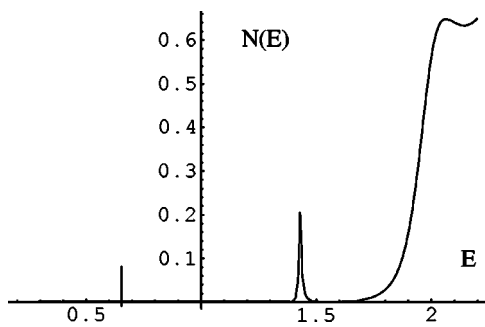


FIG. 6. Overall view of the transmission coefficient for $J = -0.2$. Atomic units (a.u.) are used.

see the influence of the second resonance $E_2 = 1.0269$, also displayed to the right in Fig. 5, while the influence of the third resonance $E_3 = 1.649$, also displayed in the right part of Fig. 4, is more pronounced. The effects on the fourth resonance $E_4 = 2.078$ are not seen individually, which means that they constitute part of the scattering background. Notice the peculiarities in the behavior of the transmission coefficient around the third resonance as displayed in the right part of Fig. 5. Two dips surround this peak: one is just below and the other is just above the real part of the second resonance energy. This is a manifestation of the interference between the resonance transmission and weak and smooth background.

The potential is still more shallow when $J = -0.2$ as seen in the rightmost part of Fig. 1. We report four resonances in Table I. The lowest resonance in this case is pushed above the second energy threshold $E_1 = 0.643$. This implies that the resonance is capable of decaying with particle emission in both left and right directions. In turn, this means that it is manifested in the transmission coefficient $N(E)$. This resonance is very narrow. The second resonance $E_2 = 1.430$ is clearly seen in the overall plot (Fig. 6). Both resonances are shown in more detail in Fig. 7. The third resonance $E_3 = 1.9835$ generates the broad structure in Fig. 6.

The figures provide detailed information on the transmission coefficient's rapid variation in the resonance region. In particular, it is demonstrated how the resonances are pushed to higher energies as the potential well becomes shallower as the potential parameter J decreases. The bound states become resonances, at first capable of decaying only to the first continuum (which corresponds to particle emission to the left, $x \rightarrow -\infty$). As J decreases further, the resonances evolve to the second continuum where they are capable of emitting

particles in both directions. Only in this situation are resonances manifested in the transmission coefficient $N(E)$. The resonance width increases in the course of this evolution. Some details of the resonance evolution deserve further study which is beyond the scope of the present work.

Another characteristic feature—the vertical tangent (cusp) behavior at the opening of the second channel—is clearly seen, although its experimental observation requires high-energy resolution, as is typical in other cases [18].

IV. CONCLUSIONS

The analytical considerations play an important role in the quantum theory of scattering. However, for a theoretically similar problem of transmission through an asymmetric potential barrier this type of approach was not applied to a due extent. We have applied analytical methods to the problem of transmission through an asymmetric potential barrier.

The transmission of an asymmetric barrier is a two-channel problem, just as a standard radial two-channel problem extensively studied in the scattering theory. This “analytical isomorphism” looks so obvious that it does not require any special proof, as soon as it is noticed. It suggests that some mapping of the one generic quantum problem onto another exists. However, construction of the mapping is non-obvious. In the present study the mapping is carried out after first casting the problems in a discrete form via expansion over some basis. This apparently technical step is essential; presently it looks unavoidable. It remains unclear how the mapping could be achieved by operating directly with differential equations.

For the one-channel problem the Siegert poles representation explicitly demonstrates meromorphic character of the scattering matrix on the complex momentum plane. For a multichannel quantum system the S matrix was shown to be a meromorphic function on the complex plane of a uniformization variable u . The barrier transmission problem belongs to the class of two-channel problems, and as such it allows quite simple explicit uniformization. A pragmatic way to implement advantages of this approach is to use the Siegert pseudostates representation. In this case all the calculations are carried out by standard methods of linear algebra.

In the present study we demonstrated how the barrier transmission problem can be solved in terms of the two-channel version of the Siegert pseudostates formalism. Within this scheme the resonance effects are treated on equal footing with background scattering and all analytical features of a two-channel quantum system are reproduced. In the nu-

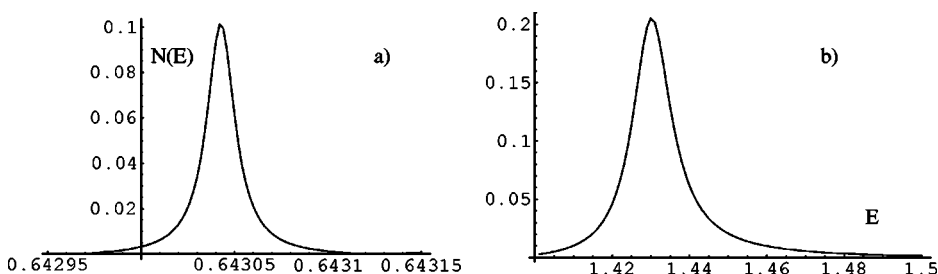


FIG. 7. The transmission coefficient $N(E)$ as a function of the energy E (a) in the vicinity of the first resonance and (b) in the vicinity of the second resonance. Atomic units (a.u.) are used.

merical application to the model potential (43) we traced the evolution of bound states and resonances as the potential depth decreases. We hope that our results are of interest both from a general point of view and as a practical method of calculation.

ACKNOWLEDGMENTS

V.N.O. acknowledges support from the Wenner Gren Foundation. The authors are thankful to O. I. Tolstikhin for reading the manuscript and making useful remarks.

-
- [1] O. I. Tolstikhin, V. N. Ostrovsky, and H. Nakamura, Phys. Rev. Lett. **79**, 2026 (1997).
 - [2] O. I. Tolstikhin, V. N. Ostrovsky, and H. Nakamura, Phys. Rev. A **58**, 2077 (1998).
 - [3] G. V. Sitnikov and O. I. Tolstikhin, Phys. Rev. A **67**, 032714 (2003).
 - [4] O. I. Tolstikhin, V. N. Ostrovsky, and H. Nakamura, Phys. Rev. A **63**, 042707 (2001).
 - [5] N. Moiseyev, P. R. Certain, and F. Weinhold, Mol. Phys. **36**, 1613 (1978).
 - [6] M. Rittby, N. Elander, and E. Brändas, Phys. Rev. A **24**, 1636 (1981); **26**, 1804 (1982).
 - [7] M. Rittby, N. Elander, and E. Brändas, Mol. Phys. **45**, 553 (1982).
 - [8] V. Ryaboy and N. Moiseyev, J. Chem. Phys. **98**, 9618 (1983).
 - [9] R. S. Friedman and D. G. Truhlar, Chem. Phys. Lett. **183**, 539 (1991).
 - [10] V. Ryaboy and R. Lefebvre, J. Chem. Phys. **99**, 9547 (1993).
 - [11] D. E. Manolopoulos and J. C. Light, Chem. Phys. Lett. **216**, 18 (1993).
 - [12] R. S. Friedman, V. Hullinger, and D. G. Truhlar, J. Phys. Chem. **99**, 3184 (1995).
 - [13] S. Shin and J. C. Light, J. Chem. Phys. **101**, 2836 (1994).
 - [14] J. Qi and J. M. Bowman, J. Chem. Phys. **104**, 7545 (1996).
 - [15] R. S. Friedman, T. C. Allison, and D. G. Truhlar, Phys. Chem. Chem. Phys. **1**, 1237 (1999).
 - [16] S. Andersson and N. Elander, J. Mol. Spectrosc. **216**, 15 (2002).
 - [17] R. G. Newton, *Scattering Theory of Waves and Particles* (McGraw-Hill, New York, 1966).
 - [18] H. R. Sadeghpour, J. L. Bohn, M. J. Cavagnero, B. D. Esry, I. I. Fabrikant, J. H. Macek, and A. R. P. Rao, J. Phys. B **33**, R93 (2002).